Available online at www.sciencedirect.com

ScienceDirect

Current Opinion in Structural Biology

Imaging of post-mortem human brain tissue using electron and X-ray microscopy

Amanda J Lewis[1], Christel Genoud[2], Mélissa Pont[1], Wilma DJ van de Berg[3], Stephan Frank[4], Henning Stahlberg[1], Sarah H Shahmoradian[5] and Ashraf Al-Amoudi[1]

Electron microscopy imaging of post-mortem human brain (PMHB) comes with a unique set of challenges due to numerous parameters beyond the researcher's control. Nevertheless, the wealth of information provided by the ultrastructural analysis of PMHB is proving crucial in our understanding of neurodegenerative diseases. This review highlights the importance of such studies and covers challenges, limitations and recent developments in the application of current EM imaging, including cryo-ET and correlative hybrid techniques, on PMHB.

Addresses
[1] Center for Cellular Imaging and NanoAnalytics (C-CINA), Biozentrum, University of Basel, Switzerland
[2] Friedrich Miescher Institute for Biomedical Research, Switzerland
[3] Department of Anatomy and Neurosciences, Section: Clinical Neuroanatomy and Biobanking, Advanced Optical Microscopy Core O2, Amsterdam Neuroscience, Amsterdam UMC, Location VU University Medical Center, Amsterdam, The Netherlands
[4] Division of Neuropathology, Institute for Medical Genetics and Pathology, University Hospital Basel, Basel, Switzerland
[5] Department of Biology and Chemistry, Paul Scherrer Institute, Villigen, Switzerland

Corresponding author:
Stahlberg, Henning (henning.stahlberg@unibas.ch)

Current Opinion in Structural Biology 2019, **58**:138–148

This review comes from a themed issue on **CryoEM**

Edited by **Matteo D Peraro** and **Ji-Joon Songo**

For a complete overview see the Issue and the Editorial

Available online 23rd July 2019

https://doi.org/10.1016/j.sbi.2019.06.003

Introduction

Neurodegenerative diseases are broad ranging and highly complex, with diverse aetiologies and frequently overlapping clinical manifestations. Among these are Alzheimer's disease (AD) and Parkinson's disease (PD), which are age-dependent disorders that are becoming increasingly prevalent worldwide [1,2,3•]. The fundamental pathophysiology of all neurodegenerative diseases is the dysfunction and ultimate loss of specialized predilected neurons and/or glial cells. Despite decades of intensive research, the molecular mechanisms underlying these diseases remain unclear, and no therapeutic strategy developed to date has been effective at combating the onset or preventing the progression of disease.

In vitro and genetic studies have provided compelling evidence about the biological and molecular processes underlying such diseases. Animal models have been used to test hypotheses for the core biological mechanisms. However, cellular and animal models are insufficient to recapitulate the entire biology of human disease [4,5]. Moreover, little is known about the morphology/ultrastructure of single neurons and glial cells in the human brain in aging and disease conditions [6,7•]. As a result, therapeutic strategies developed *in vitro* that proved to be effective in animal models have not been successfully translated to humans regarding brain diseases. Although several drugs have progressed to advanced clinical trials targeting neurodegenerative diseases such as AD, none of them have proved effective; most currently available drugs merely serve to alleviate symptoms and donot have any disease-modifying effect [8]. It is becoming increasingly clear that multiple and interlinked biological factors contribute to neuronal dysfunction and degeneration, cell–cell transmission and cell death in AD and PD. We are still missing crucial pieces of the puzzle.

In this regard, comprehensive microscopic analysis of human brain is proving to be essential toward understanding the pathological mechanisms underlying neurodegenerative disease by providing an overview of human-specific morphological, (sub)cellular features and novel pathological findings [9,10]. In fact, our understanding of human neuropathology has been largely advanced by immunohistochemistry and light microscopy (LM) analysis of post-mortem human brain (PMHB), in which misfolded protein aggregates have been identified as the major neuropathological hallmark of many neurodegenerative diseases (reviewed in Refs. [11–14]). Ultrastructural studies on PMHB using electron microscopy (EM) have been performed for decades; however, the recent 'resolution revolution' in cryo-electron microscopy (cryo-EM) [15] has allowed for higher throughput and greater sensitivity in tissue imaging and has evolved into a tool that can now monitor fine structural processes at the cellular and

molecular level in three-dimensions (3D) [16], as well as achieve high-resolution information on pathologically misfolded proteins extracted from diseased human brains [17,18]. One of the main challenges that remains in conventional EM studies is the small field of view, resulting in a long scanning time for large tissue samples as well as the difficulty in the interpretation of the images. In some cases, cellular features such as nuclei, mitochondria or cytoskeletal elements can be unambiguously recognized, whereas other structures cannot be identified purely based on their morphological signatures. Furthermore, due to the small field of view and highly crowded cellular environment, finding rare structures, such as certain pathological aggregates or cellular events in PMHB is nearly impossible when using EM alone.

As an alternative, LM, including super resolution LM (STED and PALM/STORM), volume EM methods such as serial block-face scanning electron microscopy (SBF-SEM) or focussed ion beam scanning electron microscopy (FIB-SEM), as well as X-ray microscopy (XRM), can be exploited to obtain 3D reconstructions of entire affected brain regions. Volume information from these investigations can then be used to direct higher-resolution studies using room-temperature transmission electron microscopy (TEM) or cryo-EM to relevant locations in a correlative manner. Such multimodal investigations of human brain tissue provide an essential interface and complementary approach contributing to the advancement of our understanding of the molecular mechanisms underlying neurodegeneration.

Because of the difficulty in obtaining suitable samples, ultrastructural analyses of the human brain tissue remain scarce. Biopsies of human brain are only rarely obtainable from pathological locations in very restricted clinical constellations, such as the surgical removal of epileptic foci, tumors, or necrotic tissue [19]. Most studies of human brain pathology must therefore primarily rely on the analysis of post-mortem tissue collected by brain banks using rapid autopsy protocols [20••].

While there have been many reviews in the last few years on EM imaging of non-human biological samples [21,22•], we review specifically EM and complementary modalities such as XRM techniques for imaging of post-mortem human brain. We provide example images that were recorded on postmortem human brain samples obtained as described in Suppl. Material.

Sample preparation

In contrast to studies in animal tissue, in which the conditions during euthanasia can be carefully controlled, human brain tissue can usually only be collected after death and thus post-mortem changes in the tissue are inevitable. When examining PMHB at the ultrastructural level, it can be difficult to discriminate which morphological changes are pathophysiologically relevant, and which are due to antemortem events or prolonged post-mortem delays [23,24]. In order to minimize the impact of artefacts related to post-mortem delay, sample preparation must be performed both, carefully and efficiently.

Ideally, a biological sample should be preserved directly at autopsy in a way that does not alter tissue morphology's appearance in the following imaging modality (Figure 1). In practice, this has been difficult to do, because potential artefacts to tissue morphology from each sample preparation method are difficult to recognize, primarily due to the lack of direct comparison between the tissue appearance by different imaging methods. For example, sample preparation for immunohistochemistry analysis by LM neither requires, nor typically involves, preparation protocols that preserve the detailed morphological structures otherwise necessary for EM investigation.

Room temperature sample preparation of PMHB involves the fixation, dehydration and plastic (resin) embedding of tissue, which has traditionally resulted in major ultrastructural defects at the EM level [25] (Supplementary Figure 1). Modern sample preparation protocols have been optimized for EM investigations to primarily preserve the tissue ultrastructure, and include post-fixation of PMHB samples with a mixture of paraformaldehyde and glutaraldehyde together with osmium impregnation [10,12,26–28]. This achieves excellent results for preserving the ultrastructure of both membrane and protein components of cellular architecture. Furthermore, when combined with recently developed *en-bloc* staining protocols [29], high-contrast staining throughout large tissue blocks can be achieved [30••,31•]. However, the high levels of cross-linking and heavy metal deposition used in these protocols often interfere with tissue antigenicity, rendering difficult any downstream immunolabelling studies for LM imaging. Thus, when combining LM and EM imaging methods into a single study, the initial sample preparation of choice is often a compromise to satisfy the two imaging targets. With the intensifying research into brain pathology involving LM, EM, and complementary methods such as XRM, optimized sample preparation methods for correlative studies are needed.

For cryo-EM and cryo-electron tomography (cryo-ET) of vitreous sections, termed CEMOVIS and CETOVIS respectively, the biological samples are prepared in a frozen-hydrated state that maintains its structure as close as possible to their true physiology [32]. Currently, PMHB is usually mildly chemically fixed at autopsy before high pressure freezing; however, ideally in the future, techniques will be developed to utilize unfixed

Figure 1

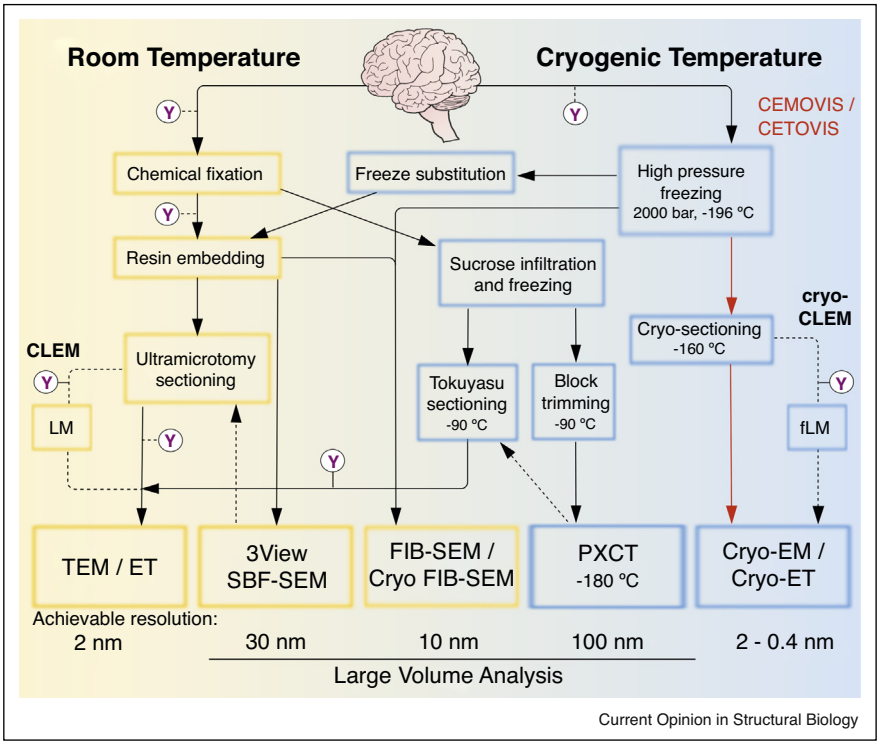

Preparation and imaging workflow for chemically fixed PMHB. Sample preparation pathways at room temperature and cryogenic temperature, leading to the major EM and X-ray imaging techniques, are shown. Currently, PMHB is mildly chemically fixed at autopsy before high pressure freezing; however, ideally in the future techniques will be developed to utilize unfixed tissue in order to avoid fixation artefacts and be imaged as close to the native state as possible. Alternative/optional pathways are depicted as dashed arrows. Room temperature preparative and imaging methods are shown in yellow, cryogenic methods in blue boxes. Points along the pathways, where immunolabelling can be applied are indicated (Y). The CEMOVIS/CETOVIS pathway is denoted by red arrows. For PXCT and SBF-SEM, return arrows demonstrate further sample processing that can occur during (SBF-SEM) or following (PXCT) large volume imaging in order to image regions of interest at a higher resolution. SBF-SEM, FIB-SEM and PXCT represent imaging methods capable of reconstructing large volumes at the cellular or tissue level as opposed to the molecular level when employing electron tomography (ET/cryo-ET) in the TEM/cryo-EM.

tissue in order to exclude any potential fixation artefacts and allow imaging as close to the native state as possible. High-pressure frozen tissue can be sectioned with a cryo-ultramicrotome, which is technically very demanding and prone to introduce cutting artifacts. Alternatively, frozen samples can be cut with a focussed ion beam scanning electron microscope (FIB-SEM), which is a relatively recently developed technique. For both these methods, the sample must remain frozen and hydrated at all times during sample preparation and imaging, which is technically difficult. Importantly, the samples do not require any staining, dehydration or resin-embedding, thereby excluding their associated artefacts. This cryo preparation enables faithful access to structural information *in situ* down to molecular resolution [33,34••].

Imaging methods

TEM, cryo-EM, and cryo-ET

Depending on the biological question, several methods for EM imaging of PMHB are available (Figure 1). TEM provides the highest resolution ultrastructural information at the nanometer scale or better. When using a tomography process where a series of images are recorded from the sample using different angles, recorded tilt series can be transformed into a 3D reconstruction by computer processing, and visualized as slices or segmented surfaces [35,36]. Repetitive or multiple copies of structures within the volumes can be averaged [37,38], resulting in 3D reconstructions of higher resolution and contrast compared to 2D images of the non-tilted samples. This allows to resolve individual structures, such as membranes, filaments, organelles, and vesicles, within a specific environment in PMHB. This was demonstrated recently in two studies using TEM imaging to analyse the ultrastructure of aggregates present in healthy and diseased human brain, revealing insights into the mechanism of ageing and PD [30••,31•].

These studies on PMHB were performed using room temperature TEM, for which the resolution of the images

was limited by the typical sample processing, that is, resin embedding and heavy metal staining (Figure 2 and Supplementary Figure 2). Here, cryo-EM and cryo-ET can overcome these resolution limits as was recently demonstrated by Guo *et al.*, who were able to discern the molecular architecture of specific protein aggregates within cultured neurons [39]. This study represents exciting prospects for future applications in PMHB. In this context, CEMOVIS and CETOVIS could offer unique solutions to resolve the molecular structure of protein aggregates *in situ* under native conditions. Some example images from CEMOVIS of PMHB are shown in Figure 2 and Supplementary Figure 2. The ultrastructure of myelin/myelin axons, mitochondria and neurofilaments is well preserved.

Figure 2

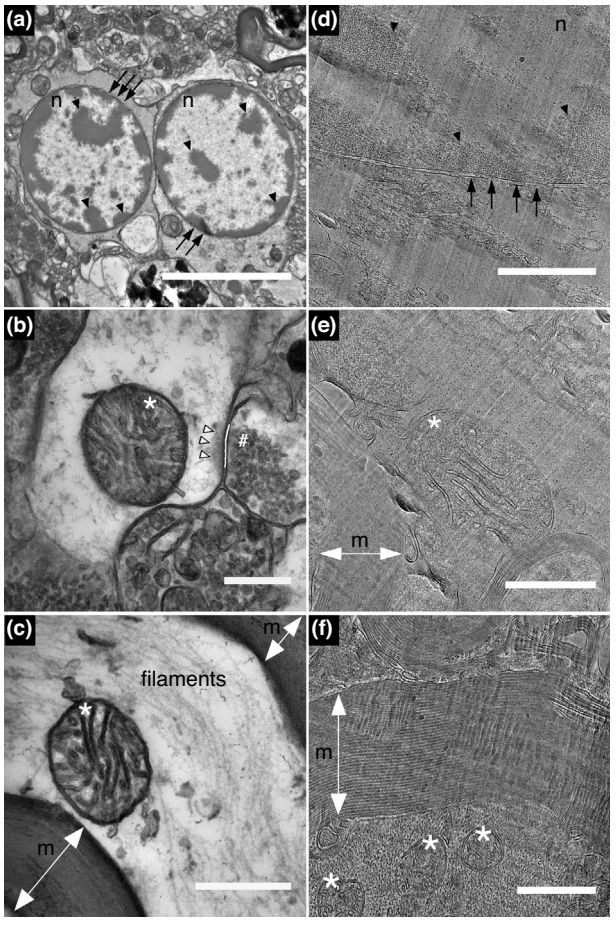

Cellular features in PMHB prepared and imaged at room temperature **(a)–(c)** or by CEMOVIS **(d)–(f)**. Chromatin in cell nuclei (n) is denoted by black arrowheads and the nuclear membrane indicated by black arrows. Mitochondria are indicated with a white asterisk and myelin sheaths (m) surrounding axons shown as white double headed arrows. Panel (b) shows a synapse between two neurons: arrow heads point to post-synaptic density, the white line indicates the synaptic cleft and the hash symbol denotes pre-synaptic vesicles. Filaments orientated laterally along the cutting axis can be seen in the axon shown in panel c. Postmortem brain tissue was fixed in 2.5% paraformaldehyde and 2% glutaraldehyde before being processed for EM as described in Ref. [30••] (a)–(c), or before being processed for CEMOVIS. Images were taken at room temperature on a T12 (FEI) electron microscope operated at 120 kV (a)–(c), or at cryogenic temperatures on a Talos electron microscope (FEI) operated at 200 kV (d)–(f). Scale bars: *a* = 5 μm; *b–f* = 500 nm.

While TEM and ET are excellent for resolving specific structures within a specific environment, they can only provide limited information for contextual and spatial information. Lower resolution techniques such as SBF-SEM, FIB-SEM, or complementary XRM offer the use of a larger surface area or volume to investigate the ultrastructure of PMHB at the cellular, rather than molecular level (Figure 1).

SBF-SEM and FIB-SEM

Both, SBF-SEM [40] and FIB-SEM [22•] utilize a scanning electron microscope (SEM) to image the surface of a fixed sample block at room temperature. Since the SEM utilizes back-scattered or secondary electrons that return from the sample block, SEM imaging requires the room-temperature sample to be fixed and extensively heavy-metal stained, to provide sufficient image signal. SBF-SEM utilizes a physical diamond-knife microtome within the vacuum chamber of the SEM to iteratively remove the upper-most surface layer, while recording surface SEM images, which are later stacked together to yield a 3D reconstruction. Recent developments in staining protocols for SBF-SEM have resulted in the fast, high-quality staining of tissue blocks in the millimeter scale [41••].

The FIB-SEM instead uses a focused ion beam of Gallium ions to iteratively remove the upper-most surface layer via ion abrasion, while a scanning electron beam records the surface images, and can be performed at both room temperature and cryogenic temperature (cryo-FIB; [42,43]). While SBF-SEM can more rapidly remove large surface layers and is therefore better suited to scan through large sample volumes, FIB-SEM can remove thinner layers of material (2–5 nm) but on much smaller areas [44]. Because of differences in beam geometry, detection system and probably gallium interaction, a higher resolution with smaller pixel size is easier to obtain with FIB-SEM. Recent advances in the image acquisition processes and device reliability has allowed for extended imaging times leading to the high-resolution reconstruction of large volumes in *Drosophila* brain, and mouse neural tissue [44].

SBF-SEM/FIB-SEM are powerful techniques to investigate larger volume and characterize the ultrastructure of the surrounding tissue. Both techniques can be combined with higher-resolution TEM: for example, once an interesting location in PMHB is identified in the SBF-SEM,

the sample can be recovered from the SEM, mounted into a conventional ultramicrotome, and a few ultrathin sections of <100 nm thickness can be cut from the volume surface. TEM imaging of these sections than can give higher-resolution (~3 nm) information on the ultrastructure of the region of interest, and ET can even be used to provide higher-resolution 3D information. Subsequently, the remainder of the block can be returned to the SBF-SEM to continue the large-volume 3D study. Such correlative SBF-SEM/TEM investigations were applied to human brain recently [30••,31•]. In this workflow, the resolution was limited by the sample preparation as metals have stained and compromised all molecular structures. A similar idea has been implemented for cryo-FIB, termed cryo-FIB lift-out [42,43]. In this method, once the region of interest has been identified, the FIB is used to mill the sample into ultra-thin vitreous lamellae that can then be imaged by cryo-TEM and cryo-ET for high-resolution ultrastructural information [45•,46]. This technique has recently been used to reveal the 3D structural state of large macrocmolecular complexes and organelles within single cells [47,48], and specific skeletal muscle junctions from tissue [49].

Meso-scale and nano-scale imaging using XRM

X-ray microscopy (XRM), a key new instrument in correlative microscopy, can generate an entire 3D view of the interior of otherwise optically opaque samples in a non-destructive way [50]. Modern XRM can produce 3D tomographic reconstructions at submicrometer isotropic resolution of biological or also non-organic samples [51,52]. Synchrotron-based XRM, given the availability of higher photon flux, allows for fast data acquisition over large tissue volumes, proving attractive for neuroscientific efforts. This technique has been used to evaluate contrast and biomarkers for PMHB samples from PD patients [53•], to visualize and count cerebellar cells in PMHB [54], to image whole brain cerebovasculature at 6-μm resolution in rats [55], and to visualize neural networks in mouse spinal cord [56]. Such complementary information can serve as valuable enrichment to histological evaluations of PMHB samples.

For using such high-energy X-rays, phase-sensitive XRM concepts such as holo-tomography, Zernike phase contrast, or coherent diffraction imaging (CDI) need to be applied because of the reduced absorption contrast of biological tissues at such energies. Ptychography is a CDI modality that involves scanning a specimen across a confined coherent illumination in a way that illuminated areas partially overlap at different scan positions [57,58]. The combination of phase images acquired at various incident angles of the beam supply the information required for 3D tomographic reconstruction of the specimen [59]. For ptychography, resolution is limited by thermal drifts, mechanical stability, and dose-dependent imaging signal-to-noise ratio, rather than a lens [60].

Ptychographic X-ray Computed Tomography (PXCT) using hard X-rays (above 5–10 keV, below 0.2–0.1 nm wavelength) is a powerful 3D synchrotron-based imaging technology [61,62] that can be applied to investigate PMHB. PXCT has the appropriate penetrative power to visualize biological materials thicker than 10 μm and spanning large regions (250 000–400 000 μm^3). Furthermore, samples can be imaged in their entirety, without additional sectioning or milling due to the greater penetration power of X-rays over electrons. The tissue does not require stain for visualizing contrast; rather, the different mass densities of intracellular and extracellular components are directly visualized [59]. As applied recently to unstained, hydrated mouse brain [63••] and PMHB [64], PXCT has proven very useful for assessing complex cellular networks in thick tissues [63••].

Recent efforts have also shown X-ray nanoholotomography to be a useful label-free imaging tool for visualizing PMHB cerebellum and neocortex using paraffin-embedded, cylindrical biopsy-punched tissue blocks, reaching a resolution of 88 nm. Cell somata, dendrites, nucleolus and nuclear envelope boundaries could be distinguished in the resulting 3D datasets [65]. In addition to the more standard resin-embedded or paraffin-embedded tissue samples used for biological imaging at the nanoscale, fully hydrated neuronal tissues such as those prepared by cryoprotection followed by slow freezing ([63••]; Tran 2018-submitted) (Supplementary Figure 3) can also be investigated by cryogenic PXCT using appropriate instrumentation such as the OMNY (tOMography Nano crYo) setup at the Paul-Scherrer Institute in Villigen, Switzerland [66]).

Common artefacts

EM analysis of PMHB tissue requires extensive sample preparation, which can cause various artefacts to tissue integrity or image quality. Most of these artefacts are not specific to PMHB and have been well documented in the literature [67–70]. These are summarized below.

Presenting together, chemical fixation and resin embedding are known to result in alteration of organelle shape and volume (e.g. swelling or shrinkage), can lead to loss of lipids from storage droplets and membranes (Supplementary Figure 1) and, if improperly done, can cause significant problems during sectioning. Heavy metals used as stains to provide contrast in the section (during either pre-embedding or post-embedding staining) are challenging to maintain soluble during tissue penetration, and can interact with some cellular compartments (e.g. the lysosomal pathway) rendering them too electron-dense for imaging [71,72]. Artefacts from cutting or sample handling such as sample compression, chatter, knife marks, section crevasses, wrinkles, folds or 'tears', are common problems in both, room temperature and cryo-sections. While these physical section defects do not always cause

Figure 3

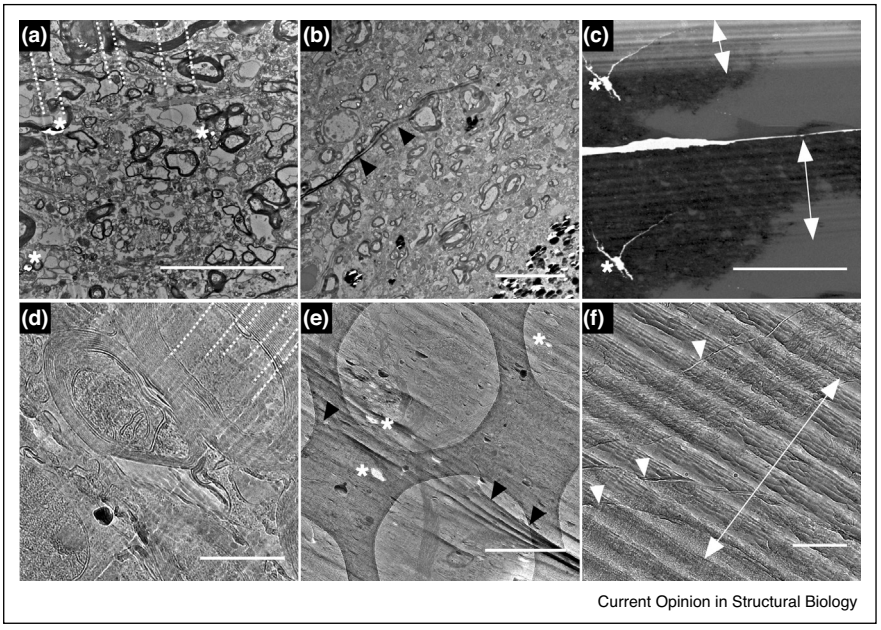

Cutting artefacts in PMHB prepared and imaged at room temperature **(a)–(c)** or by CEMOVIS **(d)–(f)**. Diamond knife marks (a), (d) are seen as tracks left in the tissue (white dotted line). Folds (b), **(e)** in the sections are indicated by black arrow heads. Chatter (c), (f) seen as hills and valleys (white double headed arrows) is created by vibrations from the diamond knife or in CEMOVIS sections by the knife surface friction. Crevasses (deep fractures in the cryosection; indicated by white arrowheads) are created by excessive compression due to the blunt knife angle used for cryo cutting, and become more prominent in cryosections thicker than 70 nm. Holes in the sections due to tearing during sectioning are indicated with white asterisks. Cutting artefacts are more pronounced in cryo-sections as compared to room temperature sections due to the cutting being performed using a dry and non-vibrating microtome knife at cryogenic temperatures. Brain tissue was fixed in 2.5% paraformaldehyde and 2% glutaraldehyde before being processed for EM as described in [30••] (a)–(c), or being processed for CEMOVIS. Images were taken at room temperature on a T12 (FEI) electron microscope operated at 120 kV (a)–(c), or at cryogenic temperatures on a Talos electron microscope (FEI) operated at 200 kV (d)–(f). Scale bars: *a*,*b* = 10 μm; *c* = 200 μm; *d*,*f* = 500 nm; *e* = 2 μm.

ultrastructural changes in cellular morphology, they can lead to distracting image artefacts (Figure 3). Cryo-sections have to be thin enough to allow transmission of the electron beam in a cryo-TEM instrument. Unfortunatly, they suffer from low structural image contrast in the cryo-EM, and the cryo-sectioning often produces pronounced artefacts, due to the cutting being performed at cryogenic temperature and the usage of a dry and non-vibrating microtome knife [67] (Figure 3). Fortunately, unlike preparation artefacts associated with conventional sample preparation, such cutting artefacts do not interfere with the physiological state of the cells and can be recognized by the trained eye, and reduced or prevented under certain conditions. The use of a focused ion beam rather than a diamond knife, cryo-FIB milling causes fewer cutting artefacts to produce 'lamellae', but the method is still novel, difficult, and inefficient, and so far only produces sections at relatively low yield [46].

Correlative imaging

Historically, the localization of specific proteins in PMHB was achieved using immunogold labelling on resin-embedded sections prepared for EM [73–75]. However, recent advances in microscopy and labelling technology, as well as sample preparation protocols have fuelled the development of hybrid approaches, termed correlative light and electron microscopy (CLEM). CLEM combines functional LM with ultrastructural contextual information from EM from a single biological event. Depending on the biological question, all CLEM approaches must be able to correlate the resulting LM to the EM images, for example, by using overlay techniques or landmark-based alignment performed either manually or facilitated by software. In some approaches the molecule of interest must be labelled to be identified by LM (e.g. using DAB-based immunohistochemistry techniques, fluorescence or genetically encoded labels) and then its ultrastructural context highlighted by EM [30••,76]. In other cases, CLEM is used to correlate *in vivo* imaging with ultrastructure in a label-free context with external cues for modality registration [77,78].

The genetically introduced fluorescent markers can be used in animal models, but are not available for studies in human brain. However, immunohistochemistry studies on PMHB can be performed either during

pre-embedding or post-embedding for CLEM studies (Figure 1). Pre-embedding antibody labelling of endogenous molecules requires careful permeabilization of the cells and membranes of the tissue, but is rewarded with good labelling efficiency. However, the permeabilization step can be detrimental to the integrity of tissue ultrastructure (reviewed in Ref. [79]). In contrast, post-embedding immuno-labelling has the drawback that the chemicals used for preparing the tissue for EM can severely limit epitope availability, thereby leading to a much lower level of labelling intensity. Despite these challenges, CLEM provides significant advantages for studies of PMHB as recently demonstrated for PD tissue [30••]. In that study, ultrathin sections of PMHB were collected alternatingly on glass slides and EM grids, which allowed the localisation of Lewy body aggregates with standard immunohistological techniques in the light microscope, followed by the use of markers in the tissue

Figure 4

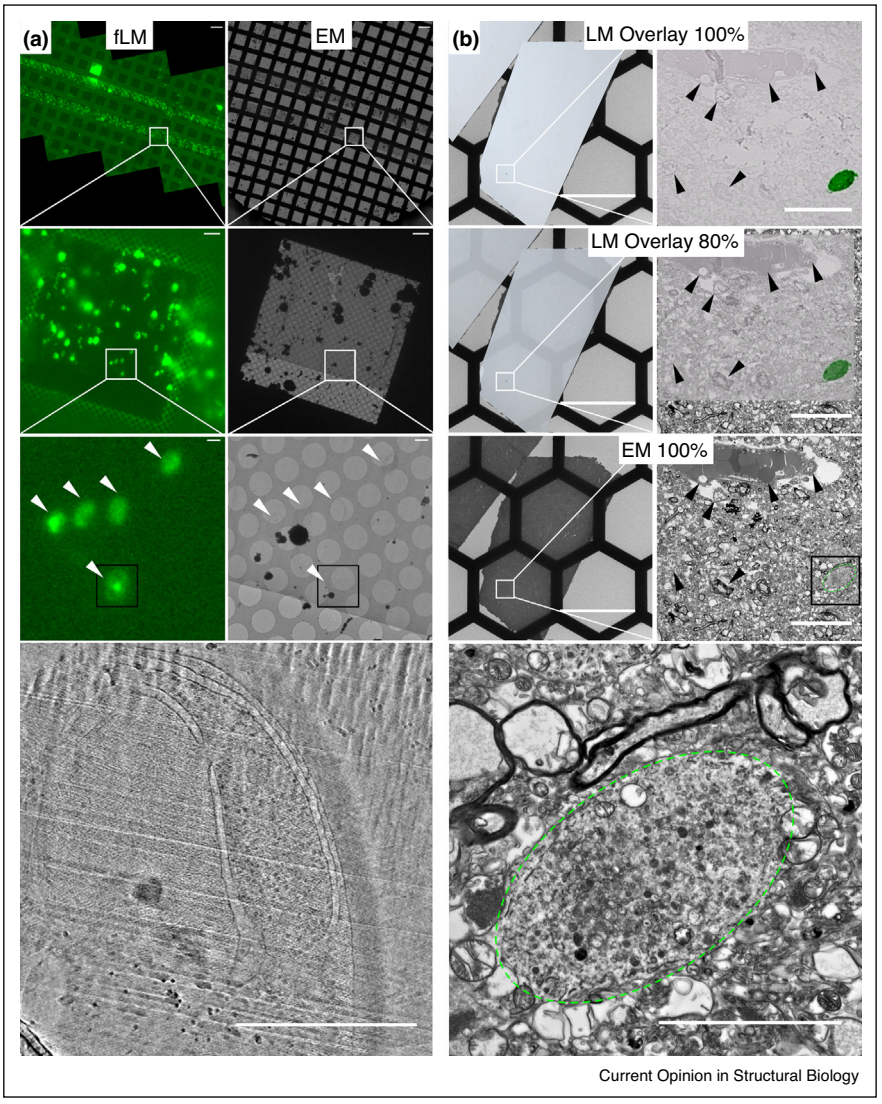

Correlative light and electron microscopy (CLEM) in cryogenic **(a)** and room temperature conditions **(b)**. (a) Vitrified ultra-thin sections of yeast cells overexpressing GFP-tagged alpha-synuclein were collected on EM grids and imaged by fluorescent microscopy (fLM) to find cells containing alpha-synuclein aggregates. Areas in white boxes are shown at higher magnifications and features identifiable in both the fluorescent and EM images are indicated with white arrowheads. Bottom: A single yeast cell (black box) is shown with EM at high magnification. (b) Ultra-thin sections of PMHB embedded in epon were collected consecutively on glass slides and EM grids. The glass slides were processed for alpha-synuclein immunoreactivity and aggregates identified by light microscopy (LM; green coloured region). Corresponding EM grids were imaged and overlaid with the LM at both low and high magnification (white boxed areas) to identify aggregates (green dashed line) in the high resolution EM landscape. Structures in the tissue identifiable in both LM and EM images were used for correlation (black arrowheads). Bottom: the Lewy body (black box), identified by LM, imaged at higher magnification in the EM. Scale bars: *a* = 100 μm, 10 μm, 2 μm and 1 μm respectively for both FM and EM images; *b* = 200 μm, 10 μm and 5 μm respectively.

such as cell nuclei, blood vessels and/or axons to accurately localize the same structures in the corresponding sections on the EM grid (Figure 4).

Array tomography

Correlative array tomography is another 3D EM approach that combines large volume data analysis with the identification of a specific subcellular structure or process of interest [26,80••,81]. While this technique has not yet been applied to PMHB, it should be adaptable for that purpose. In this method, fluorescently labelled 200–300 nm sections are serially collected on electrically conductive silicon wafers. Structures of interest are then detected by fluorescence or superresolution LM (STED, SIM, STORM, PALM), whereby the sections are then stained with metals and imaged using SEM. Instrument manufacturers are providing software to help target the high-resolution SEM image acquisition (2 nm) to the same area of the section where fluorescence was acquired. The SEM images of consecutive sections are later reconstructed into a 3D volume. The lateral resolution and possible development of multi-channel imaging provided by the superresolution LM allow for the identification of molecular identities of specific subcellular constituents with SEM providing the tissue context.

In situ Cryo-CLEM

The most native, label-guided and ultrastructurally resolving method is *in situ* cryo-CLEM of fluorescently labelled biological samples under native conditions. This approach has recently been applied to various samples [82–84,85••,86]. During transfer and imaging by cryo-fluorescence and cryo-EM, biological specimens must remain vitreous under cryogenic temperatures and in a dry environment. For that purpose, several vendors have developed light microscope cryo-stages for fluorescence LM imaging, which are now commercially available [82,87]. These systems are now including microscope control software that enables automated, tiled acquisition and image stitching of the entire sample area by cryo-fluorescence microscopy [82]. Resulting images of the frozen cryo-EM grid in form of a whole-grid image and identified locations of interest can then be transferred into a cryo-EM instrument that runs the SerialEM software [88], thus eliminating the time-consuming generation of LM–TEM overlay images before collecting high-resolution cryo-ET data. Figure 4 shows an example of the use of Leica cryo-CLEM system to study yeast cells overexpressing GFP-tagged alpha-synuclein as a PD model system.

Concluding remarks

Tissue imaging of human brain diseases must overcome the challenges of location identification, multi-scale imaging (molecules versus brain regions), and reaching sufficient resolution. Multi-resolution correlative imaging approaches are ideal for these tasks, and hold great potential towards revealing mechanisms underlying neurodegeneration. PMHB tissue is a challenging sample for studying the mechanisms of neurodegeneration, as it can be affected by the patient's age and often represents the end-stage of the disease. Little is known about which phenomenon in human brain is pathogenic, epiphenomenon, protective mechanism, or simply normal ageing. Furthermore, the possibility of tissue alterations due to extended prolonged antemortem events or post-mortem delay before sample preparation must be considered. Nevertheless, advanced EM, CLEM, and XRM of PMHB can provide unique insights into the diseased brain morphology, as no cellular or animal model is available to-date that can recapitulate the aetiopathogenesis of human neurodegenerative disease.

Conflict of interest statement

Nothing declared.

Acknowledgements

We thank Liliana Malinovska and Paula Picotti for providing the yeast cells overexpressing GFP-tagged alpha synuclein, Kenneth N. Goldie and Ariane Fecteau-LeFebvre for EM support, and the Netherlands Brain Bank for providing the PMHB tissue samples. This work was in part supported by the Swiss National Science Foundation, grant CRSII5_177195/1, the Synapsis Foundation, the Heidi Seiler Stiftung, and the NCCR TransCure.

Appendix A. Supplementary data

Supplementary material related to this article can be found, in the online version, at doi:https://doi.org/10.1016/j.sbi.2019.06.003.

References and recommended reading

Papers of particular interest, published within the period of review, have been highlighted as:

- • of special interest
- •• of outstanding interest

1. Gammon K: **Neurodegenerative disease: brain windfall**. *Nature* 2014, **515**:299-300.

2. Organisation WH: *Neurological Disorders: Public Health Challenges*. Geneva: World Health Organisation; 2006.

3. • Dorsey ER, Sherer T, Okun MS, Bloem BR: **The emerging evidence of the Parkinson pandemic**. *J Parkinson's Dis* 2018, **8**:S3-S8.

This paper describes the increasing incidence of Parkinsons's disease, highlighting it as the fastest growing neurological disease globally.

4. Newman M, Kretzschmar D, Khan I, Chen M, Verdile G, Lardelli M: **Chapter 40 – animal models of Alzheimer's disease**. In *Animal Models for the Study of Human Disease,* edn 2. Edited by Conn PM. Academic Press; 2017:1031-1085 http://dx.doi.org/10.1016/B978-0-12-809468-6.00040-1.

5. Vingill S, Connor-Robson N, Wade-Martins R: **Are rodent models of Parkinson's disease behaving as they should?** *Behav Brain Res* 2018, **352**:133-141.

6. Krause M, Theiss C, Brune M: **Ultrastructural alterations of von economo neurons in the anterior cingulate cortex in schizophrenia**. *Anat Rec (Hoboken)* 2017, **300**:2017-2024.

7. • Espay AJ, Vizcarra JA, Marsili L, Lang AE, Simon DK, Merola A, Josephs KA, Fasano A, Morgante F, Savica R *et al.*: **Revisiting protein aggregation as pathogenic in sporadic Parkinson and Alzheimer diseases**. *Neurology* 2019, **92**:329-337.

This paper calls into question the current hypotheses and therapeutic treatment strategies in neurodegeneration and challenges the discrepencies between observations in post-mortem human brain and animal models.

8. Verschuur CVM, Suwijn SR, Boel JA, Post B, Bloem BR, van Hilten JJ, van Laar T, Tissingh G, Munts AG, Deuschl G *et al.*: **Randomized delayed-start trial of levodopa in Parkinson's disease**. *N Engl J Med* 2019, **380**:315-324.

9. Laukka JJ, Kamholz J, Bessert D, Skoff RP: **Novel pathologic findings in patients with Pelizaeus-Merzbacher disease**. *Neurosci Lett* 2016, **627**:222-232.

10. Pickett EK, Rose J, McCrory C, McKenzie C-A, King D, Smith C, Gillingwater TH, Henstridge CM, Spires-Jones TL: **Region-specific depletion of synaptic mitochondria in the brains of patients with Alzheimer's disease**. *Acta Neuropathol* 2018, **136**:747-757.

11. Soto C, Pritzkow S: **Protein misfolding, aggregation, and conformational strains in neurodegenerative diseases**. *Nat Neurosci* 2018, **21**:1332-1340.

12. Henstridge CM, Sideris DI, Carroll E, Rotariu S, Salomonsson S, Tzioras M, McKenzie C-A, Smith C, von Arnim CAF, Ludolph AC *et al.*: **Synapse loss in the prefrontal cortex is associated with cognitive decline in amyotrophic lateral sclerosis**. *Acta Neuropathol* 2018, **135**:213-226.

13. Alafuzoff I, Hartikainen P: **Chapter 24 – Alpha-synucleinopathies**. In *Handbook of Clinical Neurology*, , vol 145. Edited by Kovacs GG, Alafuzoff I. Elsevier; 2018:339-353.

14. Kovacs GG: **Chapter 25 – Tauopathies**. In *Handbook of Clinical Neurology*, , vol 145. Edited by Kovacs GG, Alafuzoff I. Elsevier; 2018:355-368.

15. Kühlbrandt W: **Biochemistry. The resolution revolution**. *Science* 2014, **343**:1443-1444.

16. Ader NR, Hoffmann PC, Ganeva I, Borgeaud AC, Wang C, Youle RJ, Kukulski W: **Molecular and topological reorganizations in mitochondrial architecture interplay during Bax-mediated steps of apoptosis**. *eLife* 2019, **8**:e40712.

17. Falcon B, Zhang W, Murzin AG, Murshudov G, Garringer HJ, Vidal R, Crowther RA, Ghetti B, Scheres SHW, Goedert M: **Structures of filaments from Pick's disease reveal a novel tau protein fold**. *Nature* 2018, **561**:137-140.

18. Fitzpatrick AWP, Falcon B, He S, Murzin AG, Murshudov G, Garringer HJ, Crowther RA, Ghetti B, Goedert M, Scheres SHW: **Cryo-EM structures of tau filaments from Alzheimer's disease**. *Nature* 2017, **547**:185.

19. Mohan H, Verhoog MB, Doreswamy KK, Eyal G, Aardse R, Lodder BN, Goriounova NA, Asamoah B, Brakspear ABCB, Groot C *et al.*: **Dendritic and axonal architecture of individual pyramidal neurons across layers of adult human neocortex**. *Cereb Cortex (New York, N.Y.: 1991)* 2015, **25**:4839-4853.

20. •• Jonkman LE, Graaf YG-D, Bulk M, Kaaij E, Pouwels PJW, Barkhof F, Rozemuller AJM, van der Weerd L, Geurts JJG, van de Berg WDJ: **Normal Aging Brain Collection Amsterdam (NABCA): a comprehensive collection of postmortem high-field imaging, neuropathological and morphometric datasets of non-neurological controls**. *NeuroImage Clin* 2019, **22** 101698.
This article describes recently developed protocols for rapid autopsy collection and standardized post-mortem analysis to enable microscale to macroscale structural analysis within the same patient.

21. Koning RI, Koster AJ, Sharp TH: **Advances in cryo-electron tomography for biology and medicine**. *Ann Anat* 2018, **217**:82-96.

22. • Kopek BG, Paez-Segala MG, Shtengel G, Sochacki KA, Sun MG, Wang Y, Xu CS, van Engelenburg SB, Taraska JW, Looger LL *et al.*: **Diverse protocols for correlative super-resolution fluorescence imaging and electron microscopy of chemically fixed samples**. *Nat Protoc* 2017, **12**:916.
This paper contains detailed and easy-to-follow protocols for multiple superresolution CLEM techniques.

23. Monoranu CM, Apfelbacher M, Grünblatt E, Puppe B, Alafuzoff I, Ferrer I, Al-Saraj S, Keyvani K, Schmitt A, Falkai P *et al.*: **pH measurement as quality control on human post mortem brain tissue: a study of the BrainNet Europe consortium**. *Neuropathol Appl Neurobiol* 2009, **35**:329-337.

24. Lundström Y, Lundström P, Popova SN, Lindblom RPF, Alafuzoff I: **Detection of changes in immunohistochemical stains caused by postmortem delay and fixation time**. *Appl Immunohistochem Mol Morphol* 2019, **27**.

25. Griffiths G, Burke B, Lucocq J: *Fine Structure Immunocytochemistry*. Berlin; New York: Springer-Verlag; 1993.

26. Kay KR, Smith C, Wright AK, Serrano-Pozo A, Pooler AM, Koffie R, Bastin ME, Bak TH, Abrahams S, Kopeikina KJ *et al.*: **Studying synapses in human brain with array tomography and electron microscopy**. *Nat Protoc* 2013, **8**:1366.

27. Sittler A, Muriel M-P, Marinello M, Brice A, den Dunnen W, Alves S: **Deregulation of autophagy in postmortem brains of Machado-Joseph disease patients**. *Neuropathology* 2018, **38**:113-124.

28. Liu X-B, Schumann CM: **Optimization of electron microscopy for human brains with long-term fixation and fixed-frozen sections**. *Acta Neuropathol Commun* 2014, **2**:42.

29. Hua Y, Laserstein P, Helmstaedter M: **Large-volume en-bloc staining for electron microscopy-based connectomics**. *Nat Commun* 2015, **6**:7923.

30. •• Shahmoradian SH, Lewis AJ, Genoud C, Graff-Meyer A, Hench J, Moors T, Schweighauser G, Wang J, Goldie KN, Suetterlin R *et al.*: **Lewy pathology in Parkinson's disease consists of crowded organelles and lipid membranes**. *Nat Neurosci* 2019, **22**:1099-1109.
This paper describes novel pathologies seen in the post-mortem human brain of Parkinson's patients, providing an excellent example of the power of CLEM.

31. • Navarro PP, Genoud C, Castano-Diez D, Graff-Meyer A, Lewis AJ, de Gier Y, Lauer ME, Britschgi M, Bohrmann B, Frank S *et al.*: **Cerebral Corpora amylacea are dense membranous labyrinths containing structurally preserved cell organelles**. *Sci Rep* 2018, **8**.
This work in this paper uses correlative SBF-SEM and TEM to gain a 3-D overview of inclusions in human brain, providing clues into the normal process of ageing.

32. Al-Amoudi A, Chang JJ, Leforestier A, McDowall A, Salamin LM, Norlén LPO, Richter K, Blanc NS, Studer D, Dubochet J: **Cryo-electron microscopy of vitreous sections**. *EMBO J* 2004, **23**:3583.

33. Chlanda P, Sachse M: **Cryo-electron microscopy of vitreous sections**. In *Electron Microscopy: Methods and Protocols.* Edited by Kuo J. Humana Press; 2014:193-214 http://dx.doi.org/10.1007/978-1-62703-776-1_10.

34. •• Al-Amoudi A, Frangakis AS: **Three-dimensional visualization of the molecular architecture of cell–cell junctions in situ by cryo-electron tomography of vitreous sections**. In *Molecular Dermatology: Methods and Protocols.* Edited by Has C, Sitaru C. Humana Press; 2013:97-117 http://dx.doi.org/10.1007/978-1-62703-227-8_4.
This book chapter describes the entire CEMOVIS pipeline in detail with cruical tips to ensure high quality results.

35. Al-Amoudi A, Castano-Diez D, Devos DP, Russell RB, Johnson GT, Frangakis AS: **The three-dimensional molecular structure of the desmosomal plaque**. *Proc Natl Acad Sci U S A* 2011, **108**:6480-6485.

36. Weber MS, Wojtynek M, Medalia O: **Cellular and structural studies of eukaryotic cells by cryo-electron tomography**. *Cells* 2019, **8**.

37. Castaño-Díez D, Kudryashev M, Arheit M, Stahlberg H: **Dynamo: a flexible, user-friendly development tool for subtomogram averaging of cryo-EM data in high-performance computing environments**. *J Struct Biol* 2012, **178**:139-151.

38. Navarro PP, Stahlberg H, Castaño-Díez D: **Protocols for subtomogram averaging of membrane proteins in the dynamo software package**. *Front Mol Biosci* 2018, **5**.

39. Guo Q, Lehmer C, Martinez-Sanchez A, Rudack T, Beck F, Hartmann H, Perez-Berlanga M, Frottin F, Hipp MS, Hartl FU *et al.*:

In situ structure of neuronal C9orf72 Poly-GA aggregates reveals proteasome recruitment. *Cell* 2018, **172**:696-705 e612.

40. Denk W, Horstmann H: **Serial block-face scanning electron microscopy to reconstruct three-dimensional tissue nanostructure**. *PLoS Biol* 2004, **2**:e329.

41. •• Genoud C, Titze B, Graff-Meyer A, Friedrich RW: **Fast homogeneous en bloc staining of large tissue samples for volume electron microscopy**. *Front Neuroanat* 2018, **12**.
This paper describes a newly developed protocol for the efficient preparation of large tissue samples for volume EM, achieving high quality image stacks without comprimising staining quality in a wide variety of samples.

42. Schaffer M, Engel BD, Laugks T, Mahamid J, Plitzko JM, Baumeister W: **Cryo-focused ion beam sample preparation for imaging vitreous cells by cryo-electron tomography**. *Bio Protoc* 2015, **5**:e1575.

43. Schertel A, Snaidero N, Han H-M, Ruhwedel T, Laue M, Grabenbauer M, Möbius W: **Cryo FIB-SEM: volume imaging of cellular ultrastructure in native frozen specimens**. *J Struct Biol* 2013, **184**:355-360.

44. Xu CS, Hayworth KJ, Lu Z, Grob P, Hassan AM, García-Cerdán JG, Niyogi KK, Nogales E, Weinberg RJ, Hess HF: **Enhanced FIB-SEM systems for large-volume 3D imaging**. *eLife* 2017, **6**: e25916.

45. • Mahamid J, Schampers R, Persoon H, Hyman AA, Baumeister W, Plitzko JM: **A focused ion beam milling and lift-out approach for site-specific preparation of frozen-hydrated lamellas from multicellular organisms**. *J Struct Biol* 2015, **192**:262-269.
This paper descibes a workflow for preparing lamellas using correlative fluorescence and cyro-FIB to localize specific targets within a large multicellular volume.

46. Arnold J, Mahamid J, Lucic V, de Marco A, Fernandez J-J, Laugks T, Mayer T, Hyman AA, Baumeister W, Plitzko JM: **Site-specific cryo-focused ion beam sample preparation guided by 3D correlative microscopy**. *Biophys J* 2016, **110**:860-869.

47. Böck D, Medeiros JM, Tsao H-F, Penz T, Weiss GL, Aistleitner K, Horn M, Pilhofer M: **In situ architecture, function, and evolution of a contractile injection system**. *Science* 2017, **357**:713.

48. Mosalaganti S, Kosinski J, Albert S, Schaffer M, Strenkert D, Salomé PA, Merchant SS, Plitzko JM, Baumeister W, Engel BD *et al.*: **In situ architecture of the algal nuclear pore complex**. *NatCommun* 2018, **9**:2361.

49. Wagenknecht T, Hsieh C, Marko M: **Skeletal muscle triad junction ultrastructure by focused-ion-beam milling of muscle and cryo-electron tomography**. *Eur J Transl Myol* 2015, **25**:4823.

50. Stock SR: *MicroComputed Tomography: Methodology and Applications*. Boca Raton: CRC Press, Taylor & Francis Group; 2008.

51. Metscher BD: **MicroCT for comparative morphology: simple staining methods allow high-contrast 3D imaging of diverse non-mineralized animal tissues**. *BMC Physiol* 2009, **9**:11.

52. Karreman MA, Ruthensteiner B, Mercier L, Schieber NL, Solecki G, Winkler F, Goetz JG, Schwab Y: **Chapter 13 – Find your way with X-ray: using microCT to correlate in vivo imaging with 3D electron microscopy**. In *Methods in Cell Biology*, , vol 140. Edited by Müller-Reichert T, Verkade P. Academic Press; 2017:277-301.

53. • Carboni E, Nicolas JD, Topperwien M, Stadelmann-Nessler C, Lingor P, Salditt T: **Imaging of neuronal tissues by X-ray diffraction and X-ray fluorescence microscopy: evaluation of contrast and biomarkers for neurodegenerative diseases**. *Biomed Opt Express* 2017, **8**:4331-4347.
This paper describes the use of synchrotron radiation to visualize distinct properties in the brain tissue of Parkinsons disease patients, identifiying novel crystalline deposits and differential iron and copper levels linked to pathology.

54. Hieber SE, Bikis C, Khimchenko A, Schweighauser G, Hench J, Chicherova N, Schulz G, Müller B: **Tomographic brain imaging with nucleolar detail and automatic cell counting**. *Sci Rep* 2016, **6**:32156.

55. Zhang M-Q, Zhou L, Deng Q-F, Xie Y-Y, Xiao T-Q, Cao Y-Z, Zhang J-W, Chen X-M, Yin X-Z, Xiao B: **Ultra-high-resolution 3D digitalized imaging of the cerebral angioarchitecture in rats using synchrotron radiation**. *Sci Rep* 2015, **5**:14982.

56. Fratini M, Bukreeva I, Campi G, Brun F, Tromba G, Modregger P, Bucci D, Battaglia G, Spanò R, Mastrogiacomo M *et al.*: **Simultaneous submicrometric 3D imaging of the micro-vascular network and the neuronal system in a mouse spinal cord**. *Sci Rep* 2015, **5**:8514.

57. Dierolf M, Bunk O, Kynde S, Thibault P, Johnson I, Menzel A, Jefimovs K, David C, Marti O, Pfeiffer F: **Ptychography & lensless X-ray imaging**. *Europhys News* 2008, **39**:22-24.

58. Bunk O, Dierolf M, Kynde S, Johnson I, Marti O, Pfeiffer F: **Influence of the overlap parameter on the convergence of the ptychographical iterative engine**. *Ultramicroscopy* 2008, **108**:481-487.

59. Diaz A, Malkova B, Holler M, Guizar-Sicairos M, Lima E, Panneels V, Pigino G, Bittermann AG, Wettstein L, Tomizaki T *et al.*: **Three-dimensional mass density mapping of cellular ultrastructure by ptychographic X-ray nanotomography**. *J Struct Biol* 2015, **192**:461-469.

60. Lima E, Diaz A, Guizar-Sicairos M, Gorelick S, Pernot P, Schleier T, Menzel A: **Cryo-scanning X-ray diffraction microscopy of frozen-hydrated yeast**. *J Microsc* 2013, **249**:1-7.

61. Dierolf M, Menzel A, Thibault P, Schneider P, Kewish CM, Wepf R, Bunk O, Pfeiffer F: **Ptychographic X-ray computed tomography at the nanoscale**. *Nature* 2010, **467**:436.

62. Holler M, Diaz A, Guizar-Sicairos M, Karvinen P, Färm E, Härkönen E, Ritala M, Menzel A, Raabe J, Bunk O: **X-ray ptychographic computed tomography at 16 nm isotropic 3D resolution**. *Sci Rep* 2014, **4**:3857.

63. •• Shahmoradian SH, Tsai EHR, Diaz A, Guizar-Sicairos M, Raabe J, Spycher L, Britschgi M, Ruf A, Stahlberg H, Holler M: **Three-dimensional imaging of biological tissue by cryo X-ray ptychography**. *Sci Rep* 2017, **7**:6291.
This paper demonstrates, for the first time, non-destructive and label-free cryogenic imaging to visualize subcellular features in thick, mammalian brain samples.

64. Tran HT, Tsai EHR, Lewis A, Moors T, Bol JGJM, Rostami I, Diaz A, Joker AJ, Guizar-Sicairos M, Raabe J, Stahlberg H, van de Berg WDJ, Holler M, Shahmoradian S: *Submitted* 2019.

65. Khimchenko A, Bikis C, Pacureanu A, Hieber SE, Thalmann P, Deyhle H, Schweighauser G, Hench J, Frank S, Müller-Gerbl M *et al.*: **Hard X-ray nanoholotomography: large-scale, label-free, 3D neuroimaging beyond optical limit**. *Adv Sci* 2018, **5** 1700694.

66. Holler M, Raabe J, Diaz A, Guizar-Sicairos M, Wepf R, Odstrcil M, Shaik FR, Panneels V, Menzel A, Sarafimov B *et al.*: **OMNY—a tOMography nano crYo stage**. *Rev Sci Instrum* 2018, **89** 043706.

67. Al-Amoudi A, Studer D, Dubochet J: **Cutting artefacts and cutting process in vitreous sections for cryo-electron microscopy**. *J Struct Biol* 2005, **150**:109-121.

68. Han HM, Zuber B, Dubochet J: **Compression and crevasses in vitreous sections under different cutting conditions**. *J Microsc* 2008, **230**:167-171.

69. Walker CK, Roche JK, Sinha V, Roberts RC: **Substantia nigra ultrastructural pathology in schizophrenia**. *Schizophr Res* 2018, **197**:209-218.

70. Mollenhauer HH: **Artifacts caused by dehydration and epoxy embedding in transmission electron microscopy**. *Microsc Res Tech* 1993, **26**:496-512.

71. Neiss WF: **The electron density of light and dark lysosomes in the proximal convoluted tubule of the rat kidney**. *Histochemistry* 1983, **77**:63-77.

72. Miyawaki H: **Histochemistry and electron microscopy of iron-containing granules, lysosomes, and lipofuscin in mouse mammary glands**. *J Natl Cancer Inst* 1965, **34**:601-623.

73. Thorpe JR, Tang H, Atherton J, Cairns NJ: **Fine structural analysis of the neuronal inclusions of frontotemporal lobar degeneration with TDP-43 proteinopathy**. *J Neural Transm (Vienna)* 2008, **115**:1661-1671.

74. Arima K, Uéda K, Sunohara N, Hirai S, Izumiyama Y, Tonozuka-Uehara H, Kawai M: **Immunoelectron-microscopic demonstration of NACP/α-synuclein-epitopes on the filamentous component of Lewy bodies in Parkinson's disease and in dementia with Lewy bodies**. *Brain Res* 1998, **808**:93-100.

75. Defossez A, Beauvillain JC, Delacourte A, Mazzuca M: **Alzheimer's disease: a new evidence for common epitopes between microtubule associated protein Tau and paired helical filaments (PHF): demonstration at the electron microscope level by a double immunogold labelling**. *Virchows Archiv A* 1988, **413**:141-145.

76. Bharat TAM, Hoffmann PC, Kukulski W: **Correlative microscopy of vitreous sections provides insights into BAR-domain organization in situ**. *Structure* 2018, **26**:879-886.

77. Karreman MA, Mercier L, Schieber NL, Solecki G, Allio G, Winkler F, Ruthensteiner B, Goetz JG, Schwab Y: **Imaging single tumor cells in mice using multimodal correlative microscopy**. *Microsc Microanal* 2016, **22**:30-31.

78. Maclachlan C, Sahlender DA, Hayashi S, Molnár Z, Knott G: **Block face scanning electron microscopy of fluorescently labeled axons without using near infra-red branding**. *Front Neuroanat* 2018, **12**.

79. Schnell U, Dijk F, Sjollema KA, Giepmans BNG: **Immunolabeling artifacts and the need for live-cell imaging**. *Nat Methods* 2012, **9**:152.

80. •• Markert SM, Britz S, Proppert S, Lang M, Witvliet D, Mulcahy B, Sauer M, Zhen M, Bessereau J-L, Stigloher C: **Filling the gap: adding super-resolution to array tomography for correlated ultrastructural and molecular identification of electrical synapses at the *C. elegans* connectome**. *Neurophotonics* 2016, **3** 041802.
This paper describes a new protocol for correlative array tomography using superresultion microscopy on tissue with near-native preservation, allowing the localization of subcellular-specific features within a large tissue volume.

81. Burel A, Lavault M-T, Chevalier C, Gnaegi H, Prigent S, Mucciolo A, Dutertre S, Humbel BM, Guillaudeux T, Kolotuev I: **A targeted 3D EM and correlative microscopy method using SEM array tomography**. *Development* 2018, **145** dev160879.

82. Schorb M, Gaechter L, Avinoam O, Sieckmann F, Clarke M, Bebeacua C, Bykov YS, Sonnen AFP, Lihl R, Briggs JAG: **New hardware and workflows for semi-automated correlative cryo-fluorescence and cryo-electron microscopy/tomography**. *J Struct Biol* 2017, **197**:83-93.

83. Hampton CM, Strauss JD, Ke Z, Dillard RS, Hammonds JE, Alonas E, Desai TM, Marin M, Storms RE, Leon F *et al.*: **Correlated fluorescence microscopy and cryo-electron tomography of virus-infected or transfected mammalian cells**. *Nat Protoc* 2016, **12**:150.

84. Koning RI, Celler K, Willemse J, Bos E, van Wezel GP, Koster AJ: **Chapter 10 – Correlative cryo-fluorescence light microscopy and cryo-electron tomography of streptomyces**. In *Methods in Cell Biology*, , vol 124. Edited by Müller-Reichert T, Verkade P. Academic Press; 2014:217-239.

85. •• Sartori-Rupp A, Cordero Cervantes D, Pepe A, Gousset K, Delage E, Corroyer-Dulmont S, Schmitt C, Krijnse-Locker J, Zurzolo C: **Correlative cryo-electron microscopy reveals the structure of TNTs in neuronal cells**. *Nat Commun* 2019, **10**:342.
This study uses state-of-the-art CLEM techniques to charaterize the structural features of intra-neuronal transport mechanisms.

86. Bharat TAM, Hoffmann PC, Kukulski W: **Correlative microscopy of vitreous sections provides insights into BAR-domain organization in situ**. *Structure* 2018, **26**:879-886 e873.

87. Schorb M, Briggs JAG: **Correlated cryo-fluorescence and cryo-electron microscopy with high spatial precision and improved sensitivity**. *Ultramicroscopy* 2014, **143**:24-32.

88. Mastronarde DN: **Automated electron microscope tomography using robust prediction of specimen movements**. *J Struct Biol* 2005, **152**:36-51.